ORIGINAL PAPER

A comparative analysis of square-wave voltammetry and multi-frequency electrochemical Faradaic spectroscopy for kinetic characterisation

Franz Glaubitz[1] · Valentin Mirceski[2,3,4] · Uwe Schröder[1]

Abstract

A rigorous comparison between square-wave voltammetry (SWV) and the recently proposed multi-frequency electrochemical Faradaic spectroscopy (MEFS) is presented for both a quasireversible electrode reaction of a dissolved redox couple at a planar macroscopic electrode and a catalytic regenerative electrode mechanism (EC′ reaction scheme) by means of numerical simulations. MEFS offers fast kinetic characterisation with a minimal set of experiments, as the system is interrogated with a range of SW frequencies in a single experiment. By changing the mid-potential E_m, a critical parameter of MEFS, a broad range of standard rate constants for the heterogeneous interfacial electron transfer is accessible, ranging between 0.006 and 0.12 cm s^{-1}. In the case of the EC′ mechanism, features of the current components in both SWV and MEFS reflect the involvement of the follow-up regenerative chemical reaction (i.e. C′ catalytic step). However, for the kinetic characterisation of the EC′ mechanism, the comparative analysis suggests that SWV should be the main operating technique.

Keywords Square-wave voltammetry · Square-wave-derived techniques · Electrochemical Faradaic spectroscopy · Kinetics · Single experiment

Introduction

Square-wave voltammetry (SWV) is one of the most advanced members of the voltammetric family designed for analytical applications [1–3], mechanistic studies [4, 5], as well as kinetic and thermodynamic characterisation [6–8] of electrode processes. It combines the advantages originally offered by cyclic voltammetry and pulse voltammetric techniques, such as differential pulse voltammetry. However, despite a plethora of remarkable features, SWV is a rather complex technique, and extracting quantitative information often requires knowledge in both experiments and simulations to unlock its full potential [9]. Several new techniques have been proposed to simplify conventional SWV and advance the potential for mechanistic and kinetic characterisation of electrode processes [10–13] and some of them have already been applied comparatively to scientific problems [14, 15]. Aiming toward simplification, conventional SWV has been transformed to a kind of chronoamperometric technique, termed square-wave chronoamperometry or electrochemical Faradaic spectroscopy [16]. An important advanced variant of the latter technique is multi-frequency electrochemical Faradaic spectroscopy (MEFS) [17], in which the frequency of SW potential cycles is progressively increased during the experiment, enabling kinetic characterisation of a particular electrode reaction with a minimal set of experiments. The motivation for designing the MFES experiment stems from the consideration of the complexity of any voltammetric experiment, in which the electric current, as a typical kinetic parameter, depends on a range of parameters, some of which are hard to control rigorously during multiple experiments (e.g. the real active surface area of a single solid electrode repeatedly used). For these reasons, the estimation of intrinsic electrode kinetic parameters,

✉ Valentin Mirceski
valentin@pmf.ukim.mk

1   Institute of Biochemistry, Faculty of Natural
     Sciences and Mathematics, University of Greifswald,
     Felix-Hausdorff-Straße 4, 17489 Greifswald, Germany

2   Department of Inorganic and Analytical Chemistry,
     University of Lodz, Tamka 12, 91-403 Lodz, Poland

3   Institute of Chemistry, Faculty of Natural Sciences
     and Mathematics, Ss Cyril and Methodius University
     in Skopje, PO Box 162 1000 Skopje, North Macedonia

4   Research Center for Environment and Materials, Macedonian
     Academy of Sciences and Arts, Bul. Krste Misirkov 2,
     1000 Skopje, North Macedonia

i.e. the standard rate constant and the electron transfer coefficient, by means of a minimal set of experiments (ideally in a single experiment) seems to be important [9].

As shown in Fig. 1, the potential protocol in MEFS can be understood as a simplified version of SWV [16, 17], consisting of oppositely oriented pulses imposed on a constant potential, E_m (Fig. 1). Obviously, the underlying staircase potential variation typical for conventional SWV (Fig. 1a) is replaced by the constant mid-potential E_m in MEFS (Fig. 1b). Two opposite pulses complete a potential cycle with the duration τ, defined as $\tau = 2t_p$, where t_p is the duration of a single pulse. Conventionally, this is expressed as an SW frequency since $f = 1/\tau = 1/(2t_p)$. Importantly, in MEFS, the cycle duration is changed for progressing cycles, hence allowing the measurement of several frequencies, i.e. a frequency spectrum, in a single experiment.

Continuing our previous work [17], the present theoretical study aims to rigorously compare square-wave voltammetry and multi-frequency electrochemical Faradic spectroscopy for kinetic characterisation of electrode processes. This is achieved through simulations of a simple, quasireversible, diffusion-affected electrode reaction involving a dissolved redox couple. Additionally, we consider the well-known EC′ reaction scheme, where E represents the quasireversible electrode reac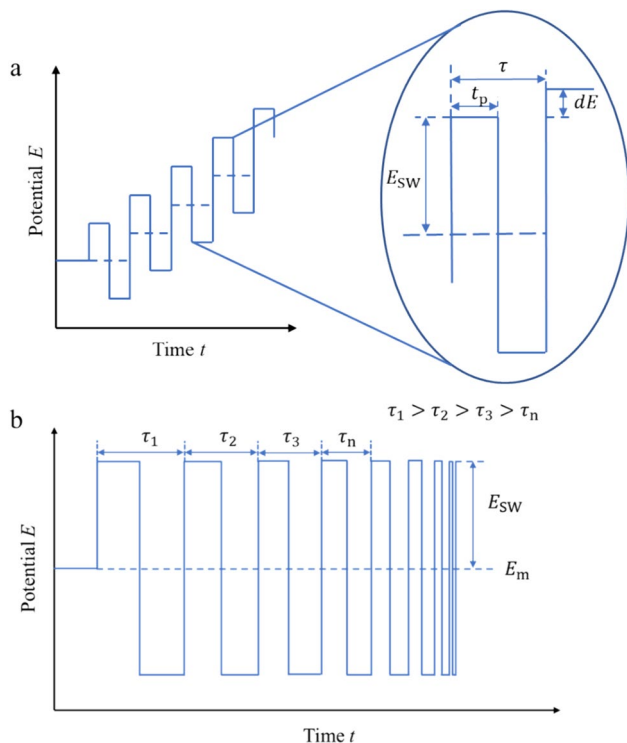tion of the dissolved redox couple, similar to the previous case. This reaction is further coupled with a follow-up, homogeneous regenerative reaction C′. The objective is to identify the advantages and disadvantages of both techniques.

Theoretical model

Quasireversible electrode reaction of a dissolved redox couple

A one-electron quasireversible electrode reaction of a solution (sol) resident redox couple (Eq. 1) at a planar electrode is considered:
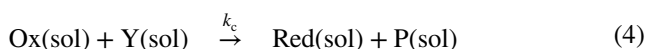
$$Red(sol) \leftrightarrows Ox(sol) + e^- \tag{1}$$

The electrode kinetics is considered in the frame of the Butler-Erdey-Gruz-Volmer equation, associated with a standard rate constant k_s and the electron transfer coefficient α [18]. At the beginning of the experiment, only the reduced form is initially present at a bulk concentration of c^*_{Red}. Furthermore, the diffusion coefficient D is assumed to be identical for both reduced and oxidised forms. A detailed insight in the used model can be found elsewhere [19, 20]. Using the step function method [20], a recurrent formula (2) for calculation of the dimensionless current Ψ is derived:

$$\Psi_m = \frac{\kappa \, \exp\left(\alpha\phi_m\right)\left\{1 - \frac{2\left[1 + \exp\left(-\phi_m\right)\right]}{\sqrt{50\pi}} \sum_{j=1}^{m-1} \Psi_j S_{m-j+1}\right\}}{1 + \frac{2\kappa \, \exp\left(\alpha\phi_m\right)}{\sqrt{50\pi}}\left[1 + \exp\left(-\phi_m\right)\right]} \tag{2}$$

where $\Psi = I/\left(FAc^*_{Red}\sqrt{Df}\right)$, $\phi = \frac{F}{RT}exp\left(E - E^{\ominus\prime}\right)$ is the dimensionless electrode potential, $\kappa = \frac{k_s}{\sqrt{Df}}$ is the dimensionless electrode kinetic parameter, and $S_m = \sqrt{m} - \sqrt{m-1}$ is the numerical integration parameter with the serial number m. For deriving the recurrent formula (2), each potential pulse is divided into 25 time compartments of identical length defined as $d = 1/(50f)$, where f is the frequency. Other symbols have their usual meaning.

Quasireversible EC′ electrode mechanism under conditions of SWV

The following set of equations describe a simple EC′ mechanism of a dissolved redox couple:

$$Red(sol) \leftrightarrows Ox(sol) + e^- \tag{3}$$

$$Ox(sol) + Y(sol) \overset{k_c}{\rightarrow} \quad Red(sol) + P(sol) \tag{4}$$

Fig. 1 Potential modulation in square-wave voltammetry (**a**) and multi-frequency electrochemical Faradaic spectroscopy (**b**)

The electrode reaction (Eq. 3) at the planar electrode is followed by a chemical reaction (Eq. 4), where the reduced species is regenerated and an electroinactive product P(sol) is formed. This reaction is associated with a pseudo-first-order rate constant k_c ($k_c = k'c*(Y)$), where k' is the second-order rate constant and $c*(Y)$ is the bulk concentration of the chemical agent Y. It is assumed that the concentration of the reducing agent Y is at least an order of magnitude greater than for the electroactive species Ox so that the overall concentration of Y at the electrode surface and in the vicinity of the electrode remains constant in the course of the experiment. The recurrent formula reads

$$\Psi_m = \frac{\kappa \exp(\alpha \phi_m)\left\{ 1 - \frac{1 + \exp(-\phi_m)}{\sqrt{\gamma}} \sum_{j=1}^{m-1} \Psi_j M_{m-j+1} \right\}}{1 + \frac{\kappa \exp(\alpha \phi_m) M_1}{\sqrt{\gamma}}\left[1 + \exp(-\phi_m) \right]} \quad (5)$$

Here, γ is the dimensionless catalytic parameter $\gamma = \frac{k_c}{f}$, $M_m = \mathrm{erf}\sqrt{\left(\frac{\gamma \times m}{50}\right)} - \mathrm{erf}\sqrt{\left(\frac{\gamma(m-1)}{50}\right)}$ is the numerical integration factor, and other symbols are identical as for Eq. (2).

Let us note that during simulations of a single SW voltammogram, the electrode kinetic parameters κ and γ have constant values for a given frequency, whereas they vary accordingly with the variation of frequency in MEFS.

Results and discussion

Simple quasireversible electrode reaction

For a simple quasireversible electrode reaction (Eq. 1), for a given electrode potential, the electrode kinetics is predominantly controlled by the dimensionless electrode kinetic parameter κ, defined as $\kappa = \frac{k_s}{\sqrt{Df}}$, where k_s is the standard rate constant, f is the SW frequency, and D is the diffusion coefficient. The electrode kinetics depends on the heterogeneous electron exchange rate, represented by k_s, relative to the rate of diffusional mass transfer, represented by the product $\sqrt{Df}$ [21]. The effect of κ on the dimensionless net peak current in conventional SWV is shown in Fig. 2a. This analysis corresponds to the comparison of a series of electrode reactions characterised by different values of κ. The dependence is sigmoidal with two plateaus, as known from the literature [20]. The upper plateau section ($\log \kappa > 1$) corresponds to the apparently reversible kinetic region where the electrode kinetics at the formal potential of the electrode reaction (i.e. the net peak potential) is virtually independent of κ, whereas the lower plateau is associated with sluggish, electrochemically irreversible electrode reactions characterised by $\log \kappa < -1.3$. The intermediate, linearly increasing section in Fig. 2a, where the dimensionless net peak-current is greatly influenced by the electrode kinetics, corresponds to the quasireversible kinetic region ($-1.3 < \log \kappa < 1$). Note
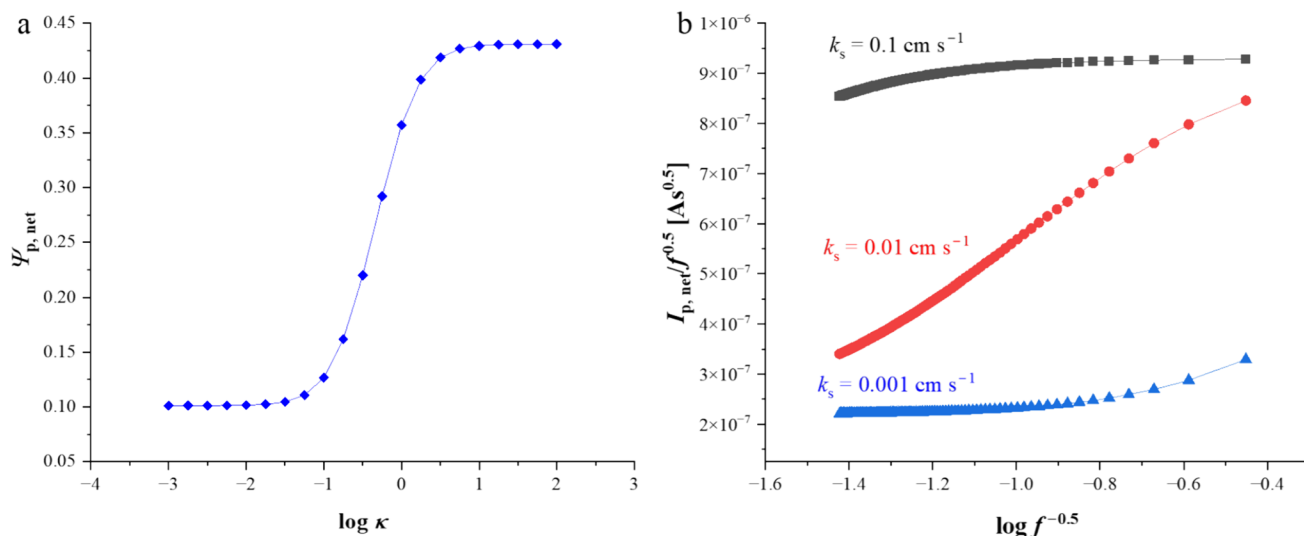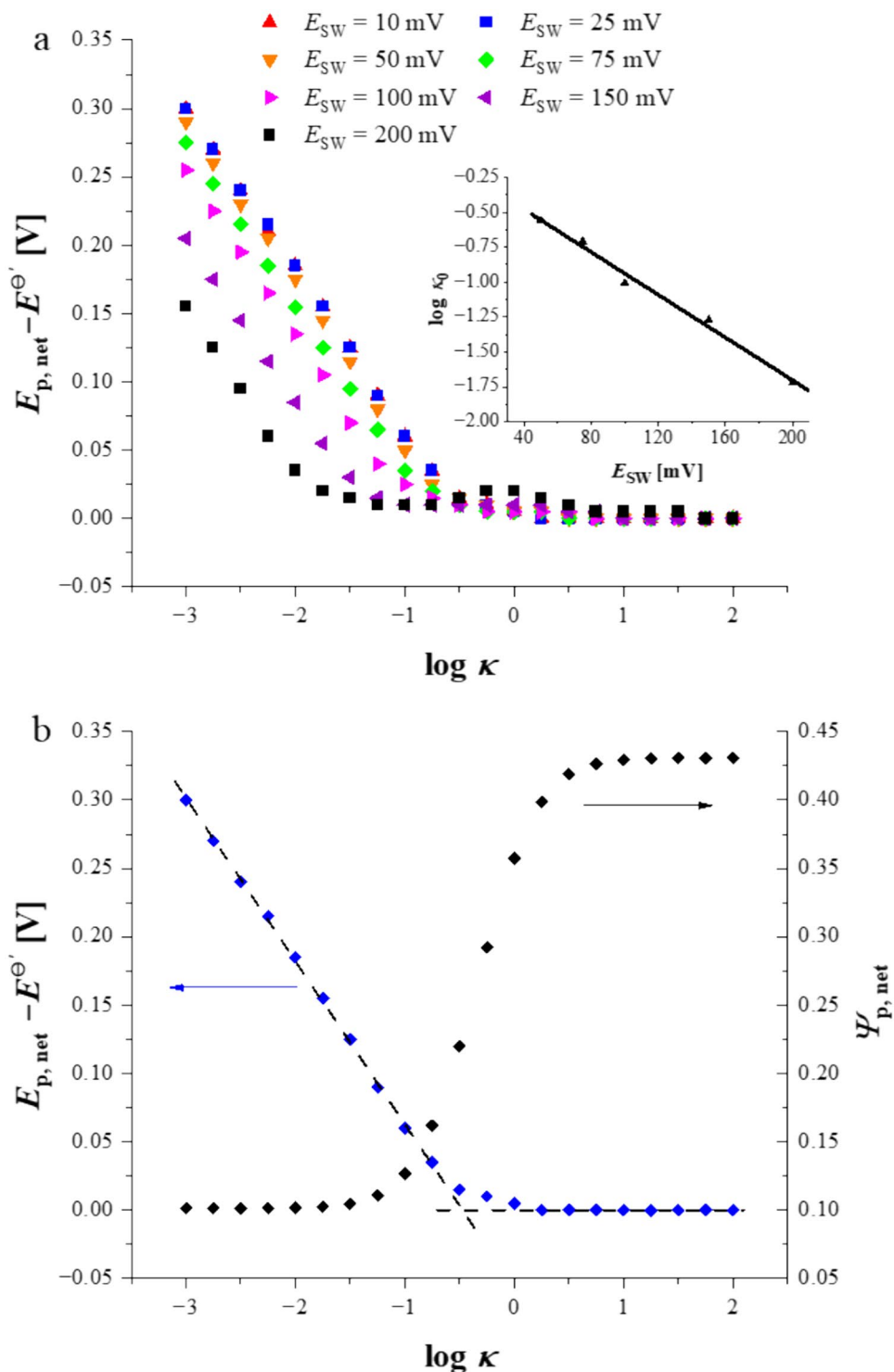
Fig. 2 Dependence of the dimensionless net peak-current $\Psi_{p,net}$ on the logarithm of the electrode kinetic parameter κ (**a**) and variation of the real current normalised by the square-root of the frequency on the logarithm of the inverse square-root of the frequency (**b**). The simulation parameters are $\Delta E = 5$ mV, $E_{SW} = 25$ mV, $\alpha = 0.5$, $D = 5 \times 10^{-6}$ cm^2 s^{-1}, $c^* = 1 \times 10^{-6}$ mol cm^{-3}, $A = 0.01$ cm^2

Table 1 Intervals for the standard rate constants for changing electrochemical reversibility under conditions identical as for Fig. 2a

Kinetic region	Inequality
Reversible section	$k_s > 10\sqrt{Df}$
Quasireversible section	$0.056\sqrt{Df} < k_s < 10\sqrt{Df}$
Irreversible section	$k_s < 0.056\sqrt{Df}$

that these kinetic intervals depend on the used amplitude, as elaborated in [22].

In the examination of a single-electrode reaction, the electrode kinetic parameter κ can be adjusted by altering the SW frequency. This analysis is depicted in Fig. 2b, where three distinct electrode reactions are analysed across the frequency range from 6 to 700 Hz. The vertical axis illustrates the ratio

Fig. 3 Dependence of the net peak-potentials (vs. the formal potential) for different square-wave amplitudes (**a**) and the overlay of the dependence of the net peak potential (blue) for $E_{SW} = 25$ mV and the dimensionless net peak current (black) on the logarithm of κ (**b**). The dashed lines in (**b**) correspond to the linear fitting functions used to determine the intersection point. The inset in (**a**) shows the linear relationship of the critical dimensionless electrode kinetic parameter associated with the inflection point of curves and the square-wave amplitude. The other conditions of simulations are identical as in Fig. 2

of the real current (I) to the corresponding frequency ($\frac{1}{\sqrt{f}}$), representing the dimensionless current. Meanwhile, the horizontal axis displays $\log(\frac{1}{\sqrt{f}})$, representing the dimensionless electrode kinetic parameter κ. Thus, each curve in Fig. 2b signifies a segment of the overall relationship between the dimensionless net peak current and the electrode kinetic parameter shown in Fig. 2a.

In instances where the electrode reaction is exceedingly fast (black curve in Fig. 2b, $k_s = 0.1$ cm s^{-1}), the ratio ($\frac{I}{\sqrt{f}}$) scarcely fluctuates with frequency, indicating the electrode reaction predominantly resides within the reversible kinetic region, as indicated by the upper plateau in Fig. 2a. For the electrode reaction with $k_s = 0.01$ cm s^{-1} (red curve in Fig. 2b), it typifies a quasireversible reaction within the specified frequency range, while the reaction possessing $k_s = 0.001$ cm s^{-1} already falls within the irreversible kinetic range (blue curve in Fig. 2b). The three kinetic intervals (irreversible, quasireversible, and reversible), in terms of the relation of the standard rate constant and SW frequency, for the conditions of Fig. 2a, are defined in Table 1.

It is important to highlight that, in conventional square-wave voltammetry, beyond examining the net peak current, one can investigate additional voltammetric features [20, 21, 23]. One such example is the net peak potential. As reversibility decreases, the net peak potential begins to shift towards higher potential values, indicating a greater driving force required for the reaction to occur. The analysis conducted for various SW amplitudes is illustrated in Fig. 3a. The inflection points of the lines in Fig. 3a signify the system's transition from quasi-reversibility to irreversibility. The inflection point can be graphically defined as the intersection point of the two regression lines, as demonstrated in Fig. 3b for the data simulated at $E_{sw} = 25$ mV.

The first regression line in Fig. 3b, with a negative slope, represents the irreversible kinetic region, while the horizontal regression line represents the quasireversible and reversible kinetic regions. Consequently, its intercept equals the formal potential of the electrode reaction ($E^{\ominus'}$) [20]. The inflection point, for a given amplitude, is linked to a critical value of the electrode kinetic parameter, κ_0. For $E_{SW} \geq 50$ mV, the critical value of the electrode kinetic parameter follows an exponential function of the amplitude. This dependence can be linearised as follows: $\log \kappa_0 = -7.64 \times 10^{-3} \times E_{SW}$ (mV) $- 0.17$ ($R^2 = 0.989$), as depicted in the inset in Fig. 3a, assuming $\alpha = 0.5$. The later dependence is slightly sensitive to the value of α, thus necessitating independent estimation of the electron transfer coefficient.

Therefore, in experimental analysis of a single-electrode reaction, one can scrutinise the variation of the net peak potential with SW frequency to determine the critical frequency (f_0) associated with the inflection point of the

dependence E_p vs. $\log(\frac{1}{\sqrt{f}})$. Knowing the critical value of κ from theory and the critical frequency from the experiment (f_0), one can estimate the standard rate constant as $k_s = \kappa_0 \sqrt{Df}$, assuming the diffusion coefficient is known.

It appears advantageous that conventional SWV allows the evaluation of various properties, providing the experimenter with the opportunity to corroborate results through cross-checking with alternative assessment methods. However, each of these methods shares the common requirement of conducting numerous experiments. Additionally, when utilising modified electrodes or when solid electrode cleaning through polishing between experiments is required, the results may be influenced by artefacts that are challenging to control, thereby affecting the precision of the estimation [9]. Furthermore, area and modification changes can affect several properties of the voltammogram as peak height and peak separation [24, 25]. This also introduces difficulties that may impede the use of direct fitting procedures.

In contrast, the MEFS facilitates rapid evaluation and characterisation of electrode reactions, ideally through a single experiment. Recent findings indicate that, for a quasireversible electrode reaction (Eq. 1), MEFS produces a maximum dimensionless net current for a given frequency within the applied frequency spectrum. Importantly, this maximum remains insensitive to both the E_{SW} and the transfer coefficient [17]. Furthermore, it has been demonstrated that this maximum is sensitive to the standard rate constant, making it exploitable for kinetic characterisation of the electrode reaction [17, 26].

However, as illustrated in Fig. 4, the maximum disappears for large (red curve, Fig. 4) or minute (blue curve, Fig. 4)
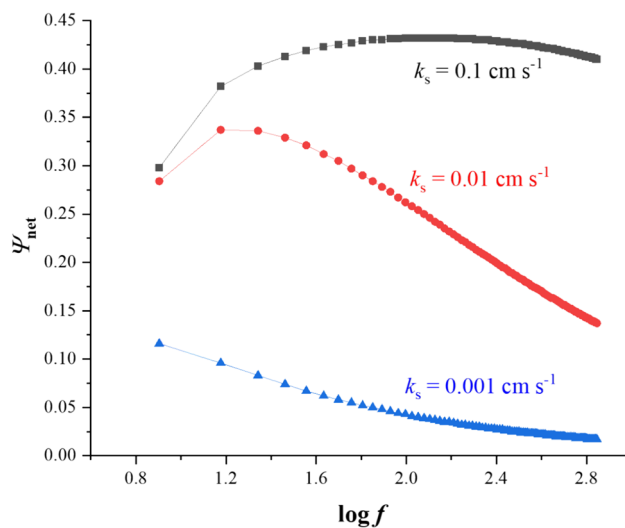

Fig. 4 Frequency spectrum in MEFS for different standard rate constants. The simulation parameters are $E_{SW} = 25$ mV, $\alpha = 0.5$, $D = 5 \times 10^{-6}$ cm^2 s^{-1}. The frequency varies from $f_0 = 8$ Hz to $f_{end} = 701$ Hz with an increment of $\Delta f = 7$ Hz

values of standard rate constants when the mid-potential equals the formal potential ($E_m = E^{\ominus'}$). Notably, the maximum can be reinstated by carefully adjusting the mid-potential and the square-wave amplitude, as depicted in Fig. 5 [16, 17]. For $E_m > E^{\ominus'}$, sluggish electrode reactions become accessible, given the greater driving force provided during the experiment (Fig. 5a). Conversely, fast electrode reactions are kinetically accessible for $E_m < E^{\ominus'}$ (Fig. 5c). Please note that the different response from a positive or a negative deviation from $E^{\ominus'}$ is based on the above-described condition of starting with a purely reduced redox couple (Eq. 1). Upon a change in E_m, standard rate constants in the range of 0.006 cm s^{-1} < k_s < 0.12 cm s^{-1} are attainable.

It is important to note that the kinetics of electrode reactions with $k_s > 0.01$ cm s^{-1} are hardly accessible in conventional SWV over the frequency interval from 8 to 700 Hz (the same frequency interval as used in MEFS), as shown in Fig. 2b. This clearly highlights the superiority of MEFS over SWV. Furthermore, while it may be tempting to choose more extreme values for E_m in MEFS to access even faster or slower reactions, this may not be feasible due to the significant increase in baseline current, potentially causing the net current response to vanish into background noise.

EC' electrode mechanism

The typical voltammetric response of a simple, EC′ catalytic process under conventional SWV conditions is illustrated in Fig. 6, displaying only the forward and backward current components. In the black curves in Fig. 6, where the chemical catalytic parameter γ is minute, the current components maintain the characteristic shape of a simple quasireversible electrode reaction. As the values of γ increase (see red and blue curves in Fig. 6), corresponding to an elevated concentration of the reducing agent Y(sol) in Eq. (4), both forward and backward current components tend to exhibit a sigmoid shape.

Consequently, two distinct kinetic regions can be identified: (i) a mixed region where the voltammetric response is influenced by the characteristics of both the electrode reaction (Eq. 3) and the catalytic chemical reaction (Eq. 4), and (ii) a purely catalytic region where the kinetics of the
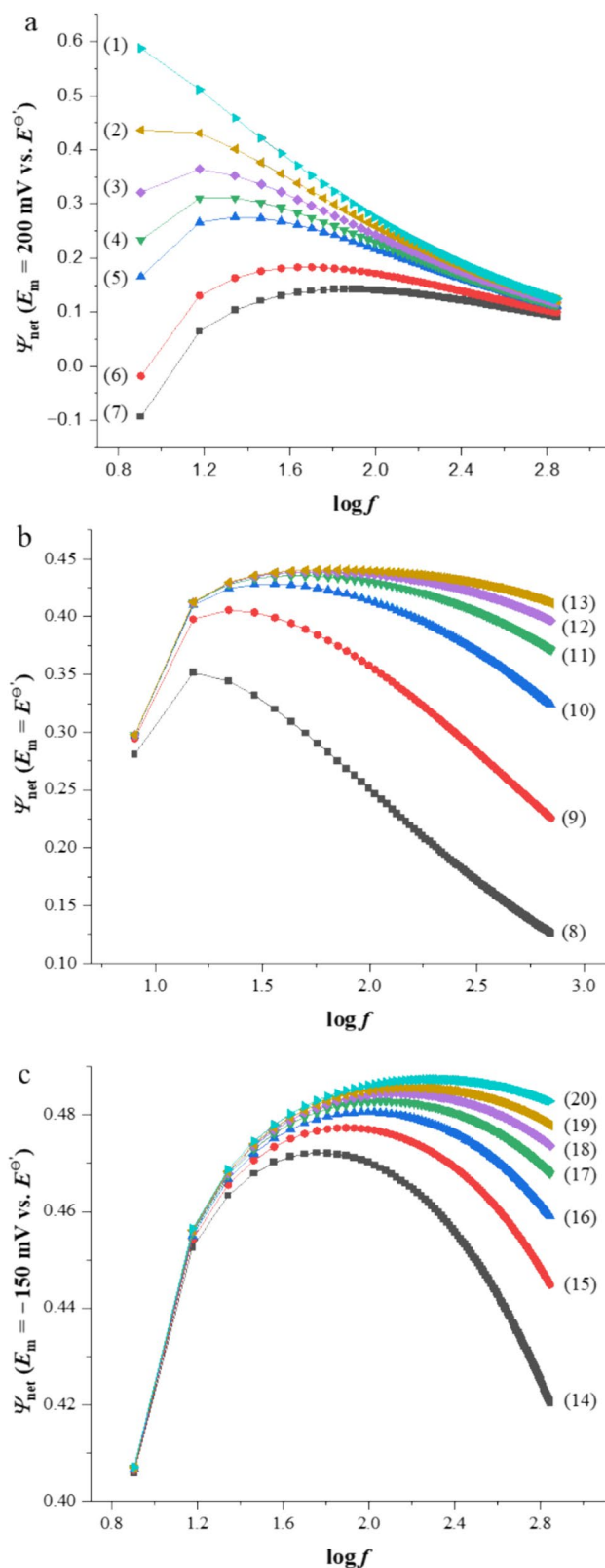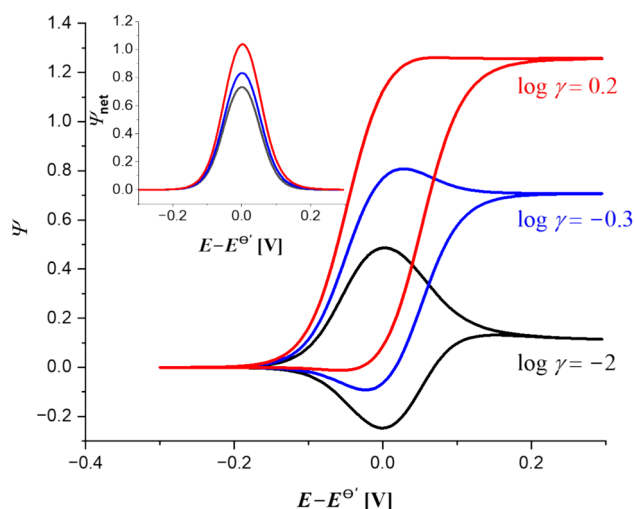
Fig. 6 Forward and backward voltammetric components of pseudo-first-order catalytic electrode reactions attributed with different values of the catalytic parameter under conditions of SWV. The inset shows the corresponding net voltammograms. Conditions of the simulations are $\kappa = 10$, $\alpha = 0.5$, $E_{SW} = 50$ mV, $\Delta E = 5$ mV

Fig. 7 Variation of the squared ratio $(\Psi_{p,net,cat}/\Psi_{p,net,diff})^2$ of the EC′ mechanism with the catalytic parameter γ. Other conditions of simulations are identical as for Fig. 6

chemical reaction (Eq. 4) prevails. Furthermore, by examining the morphological evolution of the voltammetric curves, SWV readily allows for the qualitative characterisation of the EC′ mechanism.

Regardless of the influence of a catalytic reaction, the net SW peak forms a symmetrically bell-shaped curve, clearly revealing its analytical value (inset of Fig. 6). To extract kinetic information, various approaches can be utilised. Typically, the uncatalysed reaction is studied first, and the net peak current $\Psi_{p,net}$ is obtained. Subsequently, by introducing the reducing agent Y(sol), the catalytic net peak current $\Psi_{p,net,cat}$ is measured. Simulations have demonstrated [27] that the squared ratio of ($\Psi_{p,net,cat}/\Psi_{p,net,diff}$) depends linearly on the catalytic parameter γ. When the electrochemical reaction is characterised and thus the standard rate constant is known, the linear relationship depicted in Fig. 7 suggests that the rate constant of the chemical reaction can be determined. But it is important to note that the slope of the linear functions is affected by the electrode kinetic parameter, stressing further the necessity to determine the standard rate constant of the electrode reaction prior to the analysis of the catalytic system.

Under conditions of MEFS, the behaviour of the EC′ reaction exhibits significant differences. A reaction characterised by a minute catalytic rate constant ($k_c = 10^{-5}$ s^{-1}) displays a frequency spectrum similar to that obtained for an uncatalysed reaction (compare Figs. 8a and 4). Conversely, in the
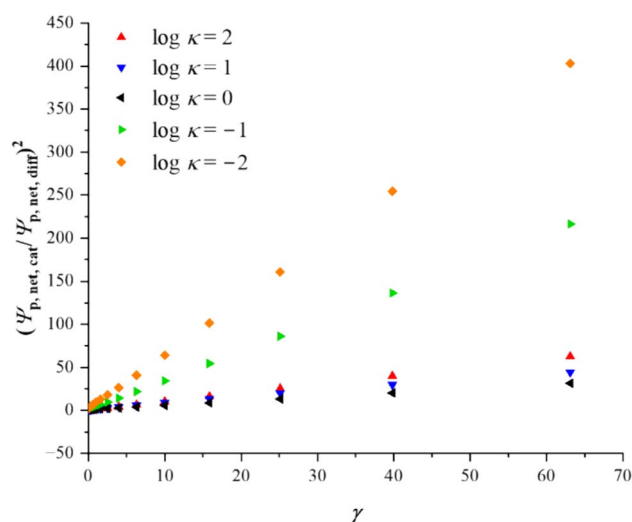
case of a reaction attributed to a higher catalytic rate constant ($k_c = 10$ s^{-1}), the influence of the catalytic step causes the maximum of the net current to vanish completely (Fig. 8b).

Similar to SWV, the evolution of the current components in MEFS is indicative for the involvement of the catalytic reaction step (compare red curves in Fig. 8). When the catalytic constant is sufficiently low, the electrode reaction (Eq. 3) dominates the features of the response. Furthermore, as the frequency increases during the MEFS experiment, the catalytic parameter $\gamma = k_c/f$ continuously decreases, rendering the role of the catalytic reaction insignificant. As detailed in our previous study [17], the maximum of the dimensionless net current component in the frequency spectrum of a simple quasireversible electrode reaction (cf. Figures 4 and 8a) is a consequence of the complex interplay of electrode kinetics, mass transfer, and expansion of the diffusion layer, primarily dependent on the overall duration of the MEFS experiment.

When the electrode reaction is fast ($k_s = 10^{-2}$ cm s^{-1}), the maximum of the dimensionless current is insensitive to the catalytic step (Fig. 9a) for $k_c < 10$ s^{-1}, suggesting that the standard rate constant might be estimated without prior knowledge of k_c. In the case of very fast electrode reactions (i.e. reversible kinetic region; $k_s = 0.1$ cm s^{-1}; Fig. 9b), the response is predominantly influenced by the kinetics of the catalytic reaction. Consequently, the evolution of the maximum is more sensitive to the rate of the catalytic reaction, implying that the determination of k_c would be possible without prior knowledge of the standard rate constant. Clearly, considering the complexity of
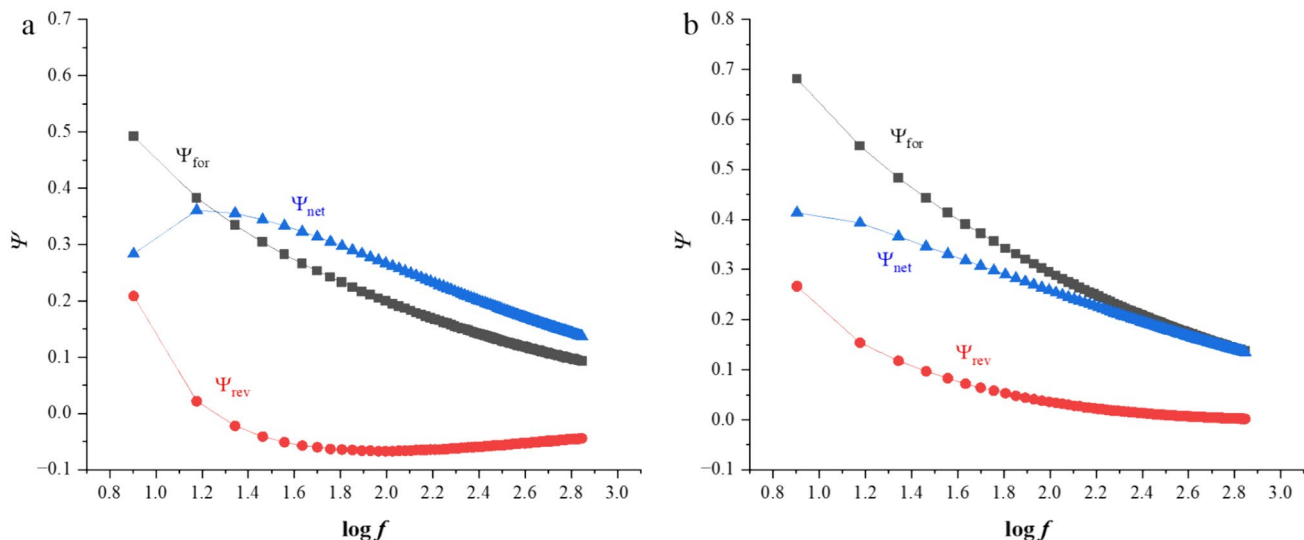
Fig. 8 Frequency spectra of two catalytic reactions associated with different pseudo-first-order rate constants of $k_c = 10^{-5}$ s^{-1} (**a**) and $k_c = 10$ s^{-1} (**b**) and a standard rate constant of $k_s = 10^{-2}$ cm s^{-1}, show- ing the forward (Ψ_{for}), reverse (Ψ_{rev}), and net (Ψ_{net}) current compo- nents. Other conditions of simulations are identical as for Fig. 4

the theoretical data, the best approach would be the fitting of experimental and theoretical data.

It should be finally emphasised that the backward current component of the MEFS is sensitive to the catalytic step, regardless of the standard rate constant of the electrode reac- tion. Therefore, the abscissa intersection of the backward

current, i.e. the critical value of the frequency when $\Psi_{rev} = 0$, depends linearly on the rate constant of the catalytic step as exemplary shown for a standard rate constant of $k_s = 0.1$ cm s^{-1} in Fig. 10. This approach is limited to catalytic con- stants of $k_c \geq 1$ s^{-1} and is additionally influenced by the exact value of the standard rate constant.
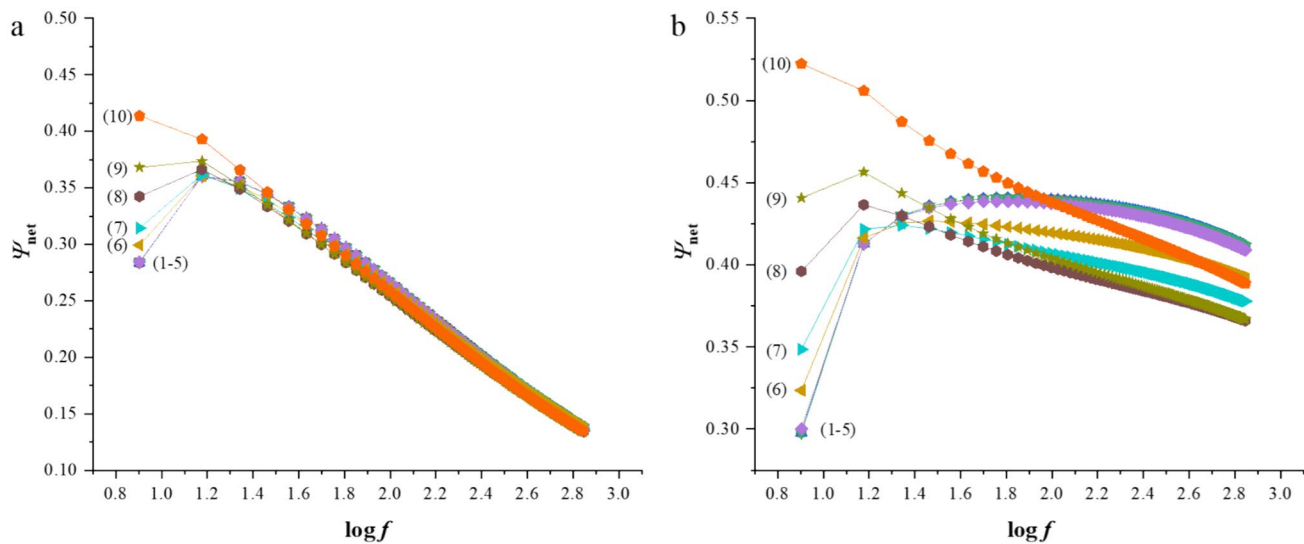

Fig. 9 Frequency spectra in MEFS for two different electro- chemical reactions attributed with $k_s = 1 \times 10^{-2}$ cm s^{-1} (**a**) and $k_s = 1 \times 10^{-1}$ cm s^{-1} (**b**) under different catalytic rate constants k_c/ s$^{-1} = 0$ (1); 0.001 (2); 0.005 (3); 0.01 (4); 0.1 (5); 1 (6); 2 (7); 4 (8); 6 (9); 10 (10). Other conditions of simulations are identical as for Fig. 4

Fig. 10 Effect of the catalytic step on the backward current of an electrochemical reaction attributed with a standard rate constant of $k_s = 0.1$ cm s^{-1} in MEFS. The inset shows the linear relationship of the abscissa of the backward current in regard to the pseudo-first-order catalytic constant. $k_c = 10$ (1); 8 (2); 6 (3); 4 (4); 2 (5) s^{-1}. The other conditions are the same as in Fig. 4
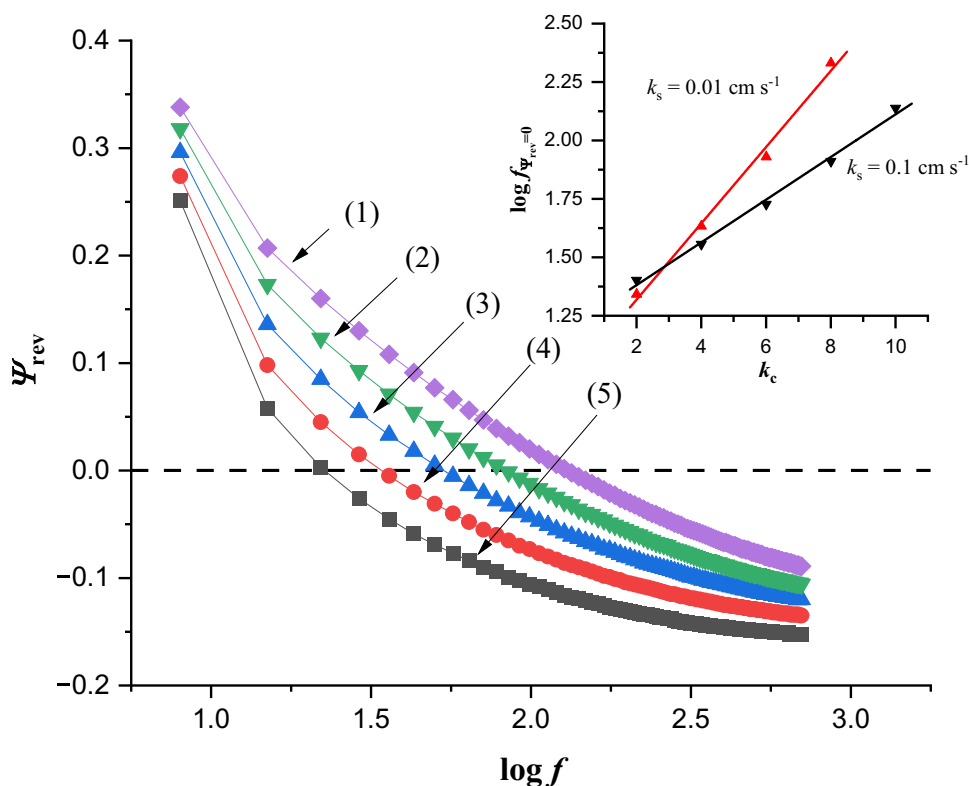
Conclusion

In this study, we continued the theoretical exploration of the recently introduced multi-frequency electrochemical Faradaic spectroscopy (MEFS) and demonstrated that careful adjustment of the mid-potential extends the accessible kinetic interval from 0.006 to 0.12 cm s^{-1} when simple quasireversible electrode reaction of a dissolved redox couple is studied. Through a comparison of MEFS and conventional square wave voltammetry (SWV) results, we concluded that MEFS can effectively reduce the required number of experiments and the overall time for pure diffusion-controlled reactions. Additionally, it is expected that the single-parameter variation in a MEFS experiment minimises variability introduced by performing multiple experiments.

We further expanded the MEFS theory to pseudo-first catalytic EC′ processes. While the significance of MEFS in this context may be less pronounced compared to uncatalysed quasireversible electrode reaction, given the complexity of results and infrequent achievement of easier-to-handle linearisations. However, for a detailed examination of EC′ mechanisms, SWV appears generally more advantageous. Nevertheless, when a fast and qualitative characterisation is required, MEFS can be easily employed.

Author contribution Franz Glaubitz: investigation, writing—original draft, writing—review and editing, visualisation, and data curation; Valentin Mirceski: supervision, writing—review and editing, and conceptualisation; Uwe Schröder: supervision, and writing—review and editing.

Declarations

Competing interests The authors declare no competing interests.

References

1. Cobb SJ, Macpherson JV (2019) Enhancing square wave voltammetry measurements via electrochemical analysis of the non-Faradaic potential window. Anal Chem 91:7935–7942. https://doi.org/10.1021/acs.analchem.9b01857
2. Kokoskarova P, Stojanov L, Najkov K et al (2023) Square-wave voltammetry of human blood serum. Sci Rep 13:1–11. https://doi.org/10.1038/s41598-023-34350-1

3. Festinger N, Smarzewska S, Mirčeski V, Ciesielski W (2021) Voltammetric determination of an anti-rheumatoid drug acemetacin on graphite flake paste electrode and glassy carbon electrode. Electroanalysis 33:314–322. https://doi.org/10.1002/elan.202060267

4. Lovrić M (2010) Square-wave voltammetry. In: Scholz F (ed) Electroanalytical Methods: Guide to Experiments and Applications. Springer, Berlin Heidelberg, pp 121–145

5. Stojanov L, Mirceski V (2023) A theoretical and experimental square-wave voltammetric study of ascorbic acid in light of multistep electron transfer mechanism. J Electrochem Soc 170:065504. https://doi.org/10.1149/1945-7111/ace030

6. Lovrić M, Komorsky-Lovric Š (1988) Square-wave voltammetry of an adsorbed reactant. J Electroanal Chem 248:239–253. https://doi.org/10.1016/0022-0728(88)85089-7

7. Dauphin-Ducharme P, Netzahualcóyotl N, Currás A-C et al (2017) Simulation-based approach to determining electron transfer rates using square-wave voltammetry. Langmuir 33:4407–4413. https://doi.org/10.1021/acs.langmuir.7b00359

8. Komorsky-Lovrić Š, Lovrić M, Scholz F (2001) Square-wave voltammetry of decamethylferrocene at the three-phase junction organic liquid/aqueous solution/graphite. Collect Czechoslov Chem Commun 66:434–444. https://doi.org/10.1135/cccc20010434

9. Mirceski V (2021) Advanced processing of electrochemical data in square-wave voltammetry. Contributions, Sec Nat Math Biotech Sci 42–43(1–2):87–94. ISSN 1857–9027

10. Mirceski V, Guziejewski D, Stojanov L, Gulaboski R (2019) Differential Square-Wave Voltammetry. Anal Chem 91:14904–14910. https://doi.org/10.1021/acs.analchem.9b03035

11. Mirceski V, Guziejewski D, Bozem M, Bogeski I (2016) Characterizing electrode reactions by multisampling the current in square-wave voltammetry. Electrochim Acta 213:520–528. https://doi.org/10.1016/j.electacta.2016.07.128

12. Mirceski V, Stojanov L, Gulaboski R (2020) Double-sampled differential square-wave voltammetry. J Electroanal Chem 872:114384. https://doi.org/10.1016/j.jelechem.2020.114384

13. Guziejewski D, Stojanov L, Zwierzz Z, Compton RG, Mirceski V (2022) Electrode kinetics from a single experiment: multi-amplitude analysis in square-wave chronoamperometry. Phys Chem Chem Phys 24:24419–24428. https://doi.org/10.1039/d2cp01888h

14. Stojanov L, Mirceski V, Peacock M Potential enhancements in commercial glucose biosensorsutilizing electrochemical Faradaic spectroscopy: analyzing thesum component in the EC' mechanism. Electroanalysis. https://doi.org/10.1002/elan.202300329

15. Stojanov L, Jovanovski V, Mirceski V (2021) Square-wave voltammetry and electrochemical Faradaic spectroscopy of a reversible electrode reaction: determination of the concentration fraction of the redox couple. Electroanalysis 33:1271–1276. https://doi.org/10.1002/ELAN.202060585

16. Jadreško D, Guziejewski D, Mirčeski V (2018) Electrochemical Faradaic spectroscopy ChemElectroChem 5:187–194. https://doi.org/10.1002/celc.201700784

17. Stojanov L, Guziejewski D, Puiu M et al (2021) Multi-frequency analysis in a single square-wave chronoamperometric experiment. Electrochem commun 124:106943. https://doi.org/10.1016/j.elecom.2021.106943

18. Bard AJ, Faulkner LR (2001) Electrochemical methods: fundamentals and applications, 2nd edn. Wiley, New York

19. O'Dea JJ, Osteryoung J, Osteryoung RA (1981) Theory of square wave voltammetry for kinetic systems. Anal Chem 53:695–701. https://doi.org/10.1021/ac00227a028

20. Mirceski V, Komorsky-Lovric S, Lovric M (2007) Square-wave voltammetry: theory and application, 1st edn. Springer, Berlin, Heidelberg

21. Mirceski V, Skrzypek S, Stojanov L (2018) Square-wave voltammetry ChemTexts 4:1–14. https://doi.org/10.1007/s40828-018-0073-0

22. Mirceski V, Laborda E, Guziejewski D, Compton RG (2013) New approach to electrode kinetic measurements in square-wave voltammetry: amplitude-based quasireversible maximum. Anal Chem 85:2022. https://doi.org/10.1021/ac4008573

23. Guziejewski D (2020) Electrode mechanisms with coupled chemical reaction — amplitude effect in square-wave voltammetry. J Electroanal Chem 870:114186. https://doi.org/10.1016/j.jelechem.2020.114186

24. Araújo DAG, Camargo JR, Pradela-Filho LA et al (2020) A lab-made screen-printed electrode as a platform to study the effect of the size and functionalization of carbon nanotubes on the voltammetric determination of caffeic acid. Microchem J 158:105297. https://doi.org/10.1016/j.microc.2020.105297

25. Zhai J, Jia Y, Ji P et al (2022) One-step detection of alpha fetal protein based on gold microelectrode through square wave voltammetry. Anal Biochem 658:114916. https://doi.org/10.1016/j.ab.2022.114916

26. Marianov AN, Kochubei AS, Roman T et al (2021) Modeling and experimental study of the electron transfer kinetics for non-ideal electrodes using variable-frequency square wave voltammetry. Anal Chem 93:10175–10186. https://doi.org/10.1021/acs.analchem.1c01286

27. Zeng J, Osteryoung RA (1986) Square wave voltammetry for a pseudo-first-order catalytic process. Anal Chem 58:2766–2771. https://doi.org/10.1021/ac00126a040

Publisher's Note Springer Nature remains neutral with regard to jurisdictional claims in published maps and institutional affiliations.